A Spectral Efficiency Design for Active IRS-assisted SWIPT System via Semidefinite Relaxation Method

Pham Viet Tuan[1], Hoang Dai Long[2], Pham Ngoc Son[3], and Mai T.P. Le[4]

[1]*University of Education, Hue University, Hue City, Vietnam,*
[2]*University of Sciences, Hue University, Hue City, Vietnam,*
[3]*Ho Chi Minh City University of Technology and Engineering, Ho Chi Minh City, Vietnam,*
[4]*University of Science and Technology, The University of Danang, Da Nang City, Vietnam*

https://doi.org/10.26636/jtit.2026.1.2267

Abstract — Active intelligent reflecting surfaces (IRS) with phase-shift and amplifier capabilities have arisen as a solution relied upon to improve spectral/energy efficiency of wireless systems, as they outperform conventional passive techniques/without IRS assistance. In this work, the simultaneous wireless information and power transfer (SWIPT) downlink is supported by an active IRS, where a multi-antenna base station (BS) broadcasts both information and power to multiple hybrid power-splitting (PS) users. The target of sum data rate maximization is to study the constraints of user energy harvesting thresholds and power transmission limitations of BS and active IRS. To tackle this complicated issue, iterative algorithms are proposed to find the optimal beamforming vector, PS coefficients, and IRS parameters, as amplification factors and phase shift. A joint optimization framework using alternating optimization, semidefinite relaxation, and non-convex approximations is used. Finally, simulation experiments are performed to assess that the proposed iterative algorithms of the active IRS scheme converge fast and achieve better sum rate results than conventional baseline schemes.

Keywords — intelligent reflecting surface, power splitting, semidefinite relaxation, simultaneous wireless information and power transfer, sum data rate

1. Introduction

Simultaneous wireless information and power transfer (SWIPT) has emerged as an effective method for powering energy-constrained devices by enabling concurrent transmission of information and energy over a single wireless channel [1]–[3]. In the meantime, active intelligent reflecting surfaces (IRS), a recent evolution of conventional passive IRS, have become crucial enablers for next-generation wireless networks, owing to their unique capability to reflect and amplify signals simultaneously [4]–[6]. Unlike passive IRS, which lacks amplification capabilities and, therefore, suffers significant cascaded path loss, active IRS effectively counteracts this limitation, enhancing signal strength during the reflection phase.

Prior research exploring IRS-assisted SWIPT primarily addressed passive IRS configurations, focusing on optimizing the reflecting elements' phase shifts to maximize energy harvesting efficiency or enhance data transmission rates [7]–[14]. For instance, several studies investigated optimizing energy efficiency and transmit power control in IRS-aided multiple-input single-output (MISO) SWIPT networks involving multiple users [7], [8]. Secure SWIPT systems employing passive IRS have also aimed at maximizing minimum secrecy rates and overall energy efficiency [11], [12]. Additionally, non-orthogonal multiple access (NOMA) schemes were employed in combination with passive IRS to further boost system performance, particularly through optimized power allocation strategies [13] and improved uplink sum rates for IoT devices [8].

Despite these advancements, the inability of passive IRS to amplify reflected signals considerably restricts their effectiveness, especially under long-distance wireless communication scenarios [2].

Recently, the introduction of active IRS has significantly mitigated these drawbacks by integrating amplification mechanisms directly with the reflecting elements. This enhancement allows active IRS to effectively overcome path loss, resulting in improvements in information transmission and energy harvesting capabilities. However, research into integrating active IRS with SWIPT remains relatively unexplored [15], [16].

A pioneering study addressing this integration, described in [15], demonstrated substantial advantages compared to passive IRS configurations, including extended wireless energy transfer range, increased sum harvested energy (SHE), and enhanced achievable data rates. Furthermore, recent findings indicate that integrating active IRS with NOMA-based SWIPT systems can further improve overall power efficiency and the minimum achievable secrecy rates [16]. Therefore, such an integration is a promising avenue for deploying robust and efficient sixth-generation (6G) architectures.

In this research, SWIPT-based communication is investigated between the transceiver of the base station (BS) with smart antennas and hybrid PS users, with the assistance of an active IRS. Two types of downlink transmit beamforming from the base station to multiple receivers may be distinguished [17], [18]. The first type is unicast transmit beamforming, where separated individual data streams are sent to multiple

Tab. 1. Summary of previous research.

Ref.	Mode	Users	IRS type	Goals	Methods	Main results
[15]	Unicast	Individual ID, EH	Active	Maximum SHE(SR) of EH(ID) users	AO, SDR, SCA, Gaussian random	Better SHE(SR) than w/o IRS
[19]	Broadcast	Only ID users	Passive	Minimum transfer power	AO, SDR, Gaussian random	Lower transfer power than w/o IRS
[20]	Unicast	Co-located ID, EH	Active	Balance SR and SHE	AO, SCA, price-based	Better results than w/o IRS
[21]	Unicast	Co-located ID, EH	Active	Minimum transfer power	AO, SDR, rank-1 approximation	Lower transfer power than passive IRS
[22]	Unicast	Individual multi-antenna ID, EH	Passive	Maximum minimum individual SR	AO, covariance matrices	Perfect/imperfect CSI, better w/o IRS
[23]	Unicast	Co-located ID, EH	Active STAR-RIS	Maximize EE	AO, SDR, FP, reinforced learning	Higher EE than baselines
Proposed	Broadcast (multicast)	Co-located ID, EH	Active	Maximize sum rate	SDR, AO, Taylor, SCA, rank-1 appr.	Higher SR than passive, w/o IRS

receivers. Otherwise, in this paper, we consider the other variety of multicast beamforming, where the base station with N antennas transmits common information $s(t)$ to multiple receivers.

In the work described in [10], only the subproblem in which the optimization of BS and hybrid user parameters is solved with fixed active IRS parameters was considered. Meanwhile, in this work, we optimize both transceivers and active IRS parameters of the overall SWIPT system, comparing the results to baselines of passive IRS assistance and a setup without IRS.

Unlike in the case of phase-shift passive IRS with unchanged signal power, both power amplification and phase change are exploited in the active IRS. Then, spectral and energy efficiency in SWIPT communication is expectedly improved with active IRS.

We present our model and the related papers in Tab. 1. The major novelty of this work is indicated as:

- The proposed SWIPT system is a combination of broadcast transmission, i.e. the same information is transferred to all users with power-splitting scheme, and active IRS assistance. Almost all other SWIPT-related works considered the unicast transmission, i.e. each user received an individual information stream.
- In the presented broadcast PS-SWIPT scheme, the sum rate target and active IRS assistance are considered, while the related broadcast IRS-aided system studied minimization of transmission power, with/without passive IRS.
- The general transformation techniques relying on semidefinite relaxation (SDR) and alternating optimization (AO) were utilized widely in the prior studies. However, we have contributed the mathematical manipulation and the efficient solution approach with Taylor and rank-1 approximations for the SDR method.

Here, we tackle the highly important issues of overcoming double fading and IoT sustainability in 6G and IoT networks. Double fading is a phenomenon where passive IRS suffers from severe path loss (product of BS-to-IRS and IRS-to-User paths). By addressing this with active IRS (with the amplification feature), we address a primary bottleneck preventing practical deployment of IRS. Additionally, SWIPT is critical for extending the lifespan of energy-constrained IoT devices without replacing their batteries. Ensuring a minimum harvested energy threshold E_k while maximizing data rates is a must for achieving sustainability in IoT.

To summarize, the main contributions of this work are outlined below.

- The goal of sum data rate maximization (SRM) (i.e., spectral efficiency) is studied, with the required parameters related to energy harvesting threshold, BS power limitation, and power budget of the active surface amplifier taken into consideration. The transceiver and active IRS parameters of BS smart beamformer and user power-splitting coefficients, the IRS phase change and amplification factors are jointly designed in the complicated non-convex SRM issue.
- We simplify the SRM problem by using the mathematical transformer and the alternating optimization (AO) technique. Then, the semidefinite relaxation (SDR) method with rank-one approximation is combined with successive convex approximation (SCA) for designing the iterative algorithm solution.
- Finally, numerical experiments are performed to analyze iteration convergence and performance compared to passive IRS and to a scenario without IRS baseline schemes. Furthermore, impacts of some system parameters are also taken into consideration.

The structure of this paper is as follows. The communication system and the SRM issue are described in Section 2. The proposed iterative algorithm for solving the SRM issue is presented in Section 3. Finally, numerical results and conclusions are shown in Sections 4 and 5, respectively.

In this paper, lowercase letters denote scalars, bold lowercase letters denote vectors, and bold uppercase letters denote matrices. In addition, $|\,x\,|$ is the absolute value of a complex scalar while $\|\,\mathbf{x}\,\|$ is the Euclidean norm of a complex vector $\mathbf{x}$. Furthemore, a diagonal matrix $\mathrm{diag}\,(\mathbf{x})$ is generated by a diagonal vector $\mathbf{x}$. The maximum eigenvalue and corresponding eigenvector of a matrix $\mathbf{X}$ are represented by $\lambda_1\,(\mathbf{X})$ and $\mathbf{v}_1$, respectively. $\mathbb{C}^{m\times n}$ is indicated as the $m \times n$ complex matrix space. Lastly, $\mathcal{CN}\left(\mu, \sigma^2\right)$ is the distribution of a circularly symmetric complex Gaussian random variable with mean μ and variance σ^2.

2. System Model Description

We study a SWIPT downlink transmission network as presented in Fig. 1. In that, a base station provided with M antennas transmits data and power to numerous hybrid PS users. The common precoding beamforming vector $\mathbf{w} \in \mathbb{C}^{M\times 1}$ is exploited at the BS and utilized for all users. The communication signal sent by the BS is indicated as $\mathbf{x} = \mathbf{w}s$ with the intended symbol s under the presumption of a zero-mean and unit variance random variable. Thus, the transmission power of the BS is calculated as $\|\mathbf{w}\|^2 \leqslant P_{\mathrm{Tx}}$ with the limited power capacity P_{Tx}.

Each PS-based hybrid user employs a power-splitting structure to simultaneously perform information decoding and energy harvesting. To improve the quality of communication, an active IRS intervention including N components is deployed. The BS-IRS link is represented by $\mathbf{G} \in \mathbb{C}^{N\times M}$ while the BS-user and IRS-user links are $\mathbf{t}_k \in \mathbb{C}^{M\times 1}$ and $\mathbf{h}_k \in \mathbb{C}^{N\times 1}$, $\forall k \in \mathcal{K} = \{1, \ldots, K\}$, respectively.

Similar to [40], at the n-th element of the active IRS, $b_n \geqslant 0$ represents the amplification coefficient and $\varphi_n \in [0, 2\pi)$ represents the phase-shift coefficient, $\forall n \in \mathcal{N} = \{1, \ldots, N\}$. As a result, the amplification impact $\mathbf{\Psi} = \mathrm{diag}\,(b_1, \ldots, b_N)$ and the phase-shift impact $\mathbf{R} = \mathrm{diag}\left(e^{j\varphi_1}, \ldots, e^{j\varphi_N}\right)$ express the amplification and reflection of the active IRS.

Accordingly, the k-th hybrid user's arriving signal, including the direct and reflecting signals, is represented as:

$$\phi_k = \left(\mathbf{t}_k^H + \mathbf{h}_k^H \mathbf{\Psi}\mathbf{R}\mathbf{G}\right)\mathbf{w}s + \mathbf{h}_k^H \mathbf{\Psi}\mathbf{R}\mathbf{z}_{\mathrm{I}} + n_k,\ \forall k \in \mathcal{K}\,. \quad (1)$$

Here, the intelligent surface with amplifying capability generates a noise $\mathbf{z}_{\mathrm{I}} \sim \mathcal{CN}\left(\mathbf{0}_N, \sigma_z^2 \mathbf{I}_N\right)$ [15], [24], [25] and the k-th hybrid user's antenna has the additive noise $n_k \sim \mathcal{CN}\left(0,\ \sigma_k^2\right)$. The k-th PS-based hybrid user splits the received signal into two streams using a power-splitting coefficient $\theta_k \in (0, 1)$, where one stream, with a power ratio of θ_k is utilized for information decoding, and the other, with a power ratio of $(1 - \theta_k)$ is used for energy harvesting [21], [26].

Although theoretical studies often model power splitting as a lossless operation, practical implementations using Wilkinson power dividers or varactor-based circuits introduce non-negligible insertion losses, such as heat on resistance elements [27], [28]. The power splitter is usually designed for a fixed impedance (e.g., 50 Ω). However, impedance mismatch incurs a loss in the harvested energy when the input impedance of the energy harvesting circuit (rectifier) changes dynamically with the input power level (i.e. is non-linear) [29]–[31]. Consequently, the ID signal part is represented as $\phi_k^{\mathrm{ID}} = \sqrt{\theta_k}\,\phi_k + v_k$ under a processing noise $v_k \sim \mathcal{CN}\left(0,\ \delta_k^2\right)$. The EH signal part is represented as $\phi_k^{\mathrm{EH}} = \sqrt{1-\theta_k}\,\phi_k$. For those reasons as [9], [40] the information rate of the k-th hybrid PS user is formulated as:

$$\Omega_k = \log_2\left(1 + \frac{\left|\left(\mathbf{t}_k^H + \mathbf{h}_k^H \mathbf{\Psi}\mathbf{R}\mathbf{G}\right)\mathbf{w}\right|^2}{\sigma_z^2 \|\mathbf{h}_k^H \mathbf{\Psi}\mathbf{R}\|^2 + \sigma_k^2 + \frac{\delta_k^2}{\theta_k}}\right),\ \forall k \in \mathcal{K}\,, \quad (2)$$

and the received energy with the presumption of completed efficiency conversion is given by:

$$\Upsilon_k = (1 - \theta_k)\left(\left|\left(\mathbf{t}_k^H + \mathbf{h}_k^H \mathbf{\Psi}\mathbf{R}\mathbf{G}\right)\mathbf{w}\right|^2 + \sigma_z^2 \left\|\mathbf{h}_k^H \mathbf{\Psi}\mathbf{R}\right\|^2\right), \forall k\,. \quad (3)$$

3. Joint Active IRS and Transceivers Design

Here, the sum rate maximization problem for active IRS-aided SWIPT system is introduced and an efficient iteration solution algorithm is proposed. The target is to optimize spectral efficiency by jointly designing the parameters of transceivers and active IRS.

Unlike in [9], [40], here, the BS beamformer, the hybrid users PS coefficients, and the active IRS's amplification and phase-shifting coefficients are degined jointly using a novel spectral efficiency maximization problem (P1) which can be formulated as:

$$\underset{\{\mathbf{w},\theta_k,\varphi_n,b_n\}}{\text{maximize}} \sum_{k=1}^{K} \log_2\left(1 + \frac{\left|\left(\mathbf{t}_k^H + \mathbf{h}_k^H \mathbf{\Psi}\mathbf{R}\mathbf{G}\right)\mathbf{w}\right|^2}{\sigma_z^2 \left\|\mathbf{h}_k^H \mathbf{\Psi}\mathbf{R}\right\|^2 + \sigma_k^2 + \frac{\delta_k^2}{\theta_k}}\right) \quad (4a)$$

subject to: (4b)

$$(1 - \theta_k)\left(\begin{array}{l}\left|\left(\mathbf{t}_k^H + \mathbf{h}_k^H \mathbf{\Psi}\mathbf{R}\mathbf{G}\right)\mathbf{w}\right|^2 \\ +\sigma_z^2 \left\|\mathbf{h}_k^H \mathbf{\Psi}\mathbf{R}\right\|^2\end{array}\right) \geqslant E_k, \forall k \quad (4c)$$

$$\|\mathbf{w}\|^2 \leqslant P_{\mathrm{Tx}} \quad (4d)$$

$$\|\mathbf{\Psi}\mathbf{R}\mathbf{G}\mathbf{w}\|^2 + \sigma_z^2 \|\mathbf{\Psi}\mathbf{R}\|^2 \leqslant P_{\mathrm{I}} \quad (4e)$$

$$1 \geqslant \theta_k \geqslant 0,\ \forall k \in \mathcal{K} \quad (4f)$$

$$\varphi_n \in [0, 2\pi)\,,\ \forall n \in \mathcal{N}. \quad (4g)$$

The target formulated in (4a) is the maximization of the total information rate of hybrid users. We consider a system suitable for energy-constrained applications, such as sensor networks, where only the base station possesses a reliable power supply. The receivers must therefore sustain their operations by replenishing energy via the signals received from the active IRS-assisted base station. In the constraint (4b), the amount of harvested energy is larger than the minimum required EH threshold, E_k which provides enough power for basic operations, similar to [13], [32], [33]. Constraints (4d)

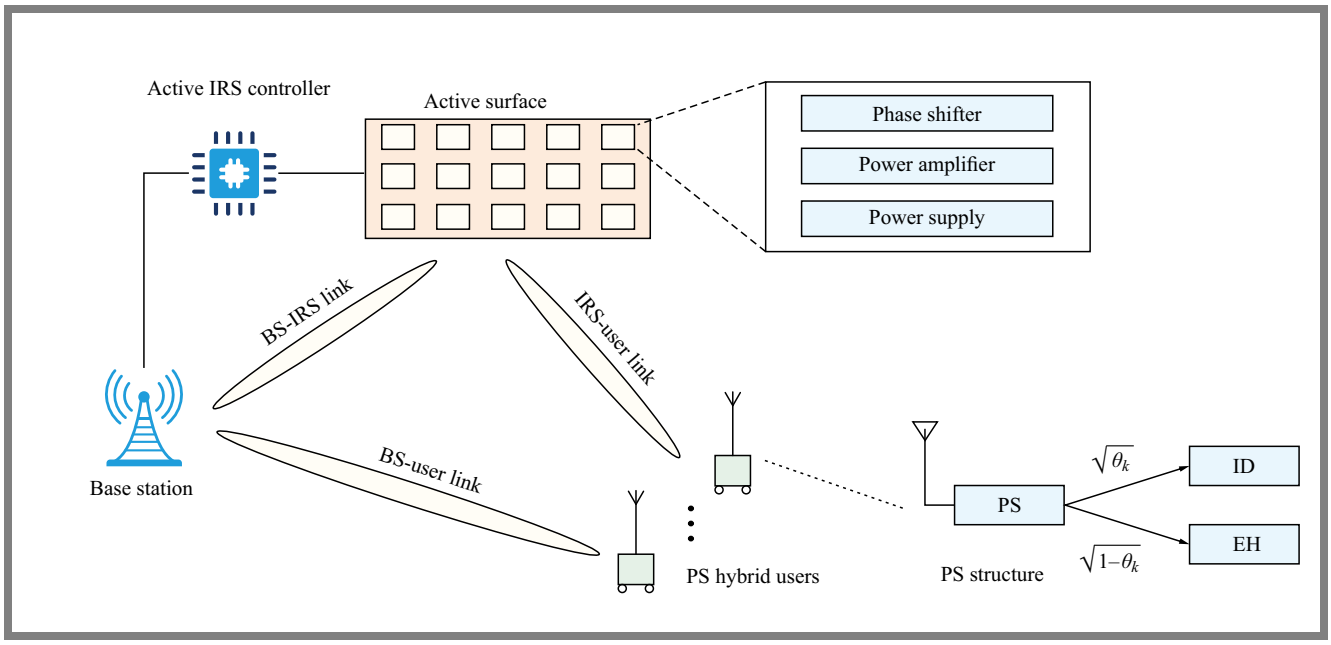

Fig. 1. Illustration of SWIPT communication with an active IRS intercession and PS hybrid users.

and (4e) introduce the maximum powers of the BS, P_{Tx}, and the active IRS, P_{I}.

In this paper, we consider that the amplifier units of active IRS elements share a common power source, as in [4], [21], [25], [34]. Thus, the amplification power of all active IRS elements is limited by the total power constraint, as illustrated in constraint (4e). Otherwise, in the other model of active IRS, each active IRS reflecting element is equipped with its own power source and independently controlled power. Therefore, the maximum amplification factor of each element is limited by its individual amplification power budget. This is a challenging problem we will aim to consider in our future research.

Formulas (4f) and (4g) present the intervals of PS coefficients at the hybrid users and the phase shifts at the active IRS components, respectively. The idea relied upon to solve the spectral efficiency maximization problem consists in combining alternating optimization, SCA iteration, and SDR with rank-one relaxation. We first separate the coupled variables $\{\mathbf{w}, \theta_k, \varphi_n, b_n\}$ into two sets of transceiver parameters $\{\mathbf{w}, \theta_k\}$ and active IRS parameters $\{\varphi_n, b_n\}$, then the SDR method is applied to solve subproblems.

3.1. Solving the Transceiver Parameters Sub-problem

As stated in (4a), the total sum rate function is very complicated due to the couple of transceiver parameters of beamforming vector, PS factors $\{\mathbf{w}, \theta_k\}$ and the SINR ratios inside $\sum_{k=1}^{K} \log_2(\cdot)$ function. Thus, we simplify the objective function by inserting the auxiliary variables $\{u_k,\ v_k\}$ as formulas (5a), (5b), and (5c) where two problems have the same maximum value (please see the proof in Appendix A). Then, we transform into the equivalent problem (P2) as:

$$\max_{\substack{\mathbf{w},\theta_k,\\ u_k,v_k}} \sum_{k=1}^{K} \log_2\left(1+\frac{u_k}{v_k+\sigma_k^2}\right) \tag{5a}$$

$$\text{s.t.: } \left|\left(\mathbf{t}_k^H+\mathbf{h}_k^H\boldsymbol{\Psi}\mathbf{R}\mathbf{G}\right)\mathbf{w}\right|^2 \geqslant u_k, \forall k\in\mathcal{K} \tag{5b}$$

$$\sigma_z^2\left\|\mathbf{h}_k^H\boldsymbol{\Psi}\mathbf{R}\right\|^2+\frac{\delta_k^2}{\theta_k}\leqslant v_k, \forall k\in\mathcal{K} \tag{5c}$$

$$\left(\begin{array}{l}\left|\left(\mathbf{t}_k^H+\mathbf{h}_k^H\boldsymbol{\Psi}\mathbf{R}\mathbf{G}\right)\mathbf{w}\right|^2\\ +\sigma_z^2\left\|\mathbf{h}_k^H\boldsymbol{\Psi}\mathbf{R}\right\|^2\end{array}\right)\geqslant\frac{E_k}{(1-\theta_k)}, \forall k\in\mathcal{K} \tag{5d}$$

$$\|\mathbf{w}\|^2\leqslant P_{\mathrm{Tx}} \tag{5e}$$

$$\|\boldsymbol{\Psi}\mathbf{R}\mathbf{G}\mathbf{w}\|^2+\sigma_z^2\|\boldsymbol{\Psi}\mathbf{R}\|^2\leqslant P_{\mathrm{I}} \tag{5f}$$

$$1\geqslant\theta_k\geqslant 0,\ \forall k\in\mathcal{K}. \tag{5g}$$

For constraint (5b), we then convert the energy harvesting constraints as:

$$\left|\left(\mathbf{t}_k^H+\mathbf{h}_k^H\boldsymbol{\Psi}\mathbf{R}\mathbf{G}\right)\mathbf{w}\right|^2=\mathrm{Tr}\left(\mathbf{T}_k\mathbf{w}\mathbf{w}^H\right), \tag{6}$$

where

$$\mathbf{T}_k=\left(\mathbf{t}_k^H+\mathbf{h}_k^H\boldsymbol{\Psi}\mathbf{R}\mathbf{G}\right)^H\left(\mathbf{t}_k^H+\mathbf{h}_k^H\boldsymbol{\Psi}\mathbf{R}\mathbf{G}\right).$$

For constraint (5c), the function exhibits convexity with respect to $\{\theta_k, v_k\}$.

For constraints (5d), we express as follows:

$$\mathrm{Tr}\left(\mathbf{T}_k\mathbf{w}\mathbf{w}^H\right)+\sigma_z^2\left\|\mathbf{h}_k^H\boldsymbol{\Psi}\mathbf{R}\right\|^2\geqslant\frac{E_k}{(1-\theta_k)}. \tag{7}$$

For constraint (5e), $\mathrm{Tr}\left(\mathbf{w}\mathbf{w}^H\right)\leqslant P_{\mathrm{Tx}}$ and constraint (5f), we denote $\mathbf{H}=\left(\boldsymbol{\Psi}\mathbf{R}\mathbf{G}\right)^H\left(\boldsymbol{\Psi}\mathbf{R}\mathbf{G}\right)$ and formulate:

$$\mathrm{Tr}\left(\left(\boldsymbol{\Psi}\mathbf{R}\mathbf{G}\right)^H\left(\boldsymbol{\Psi}\mathbf{R}\mathbf{G}\right)\mathbf{w}\mathbf{w}^H\right)+\sigma_z^2\|\boldsymbol{\Psi}\mathbf{R}\|^2\leqslant P_{\mathrm{I}}. \tag{8}$$

For the objective function, we analyze:

$$\log_2\left(1+\frac{u_k}{v_k+\sigma_k^2}\right) = \log_2\left(v_k+u_k+\sigma_k^2\right)-\log_2\left(v_k+\sigma_k^2\right). \tag{9}$$

By exploiting SDR method, we transform the beamforming vector to the matrix variables $\mathbf{w}$ by the useful transformation $\mathbf{W}=\mathbf{w}\mathbf{w}^H$, $\mathbf{w}\neq\mathbf{0}$ where $\mathbf{W}\succeq 0$, $\text{rank}\,(\mathbf{W})=1$ [35].

$$\max_{\substack{\mathbf{W},\theta_k,\\ u_k,v_k}}\ \sum_{k=1}^{K}\left[\log_2\left(v_k+u_k+\sigma_k^2\right)-\log_2\left(v_k+\sigma_k^2\right)\right] \tag{10a}$$

$$\text{s.t.: } u_k-\text{Tr}\left(\begin{array}{c}\left(\mathbf{t}_k^H+\mathbf{h}_k^H\mathbf{\Psi}\mathbf{R}\mathbf{G}\right)^H\\ \left(\mathbf{t}_k^H+\mathbf{h}_k^H\mathbf{\Psi}\mathbf{R}\mathbf{G}\right)\mathbf{W}\end{array}\right)\leqslant 0,\forall k\in\mathcal{K} \tag{10b}$$

$$\sigma_z^2\left\|\mathbf{h}_k^H\mathbf{\Psi}\mathbf{R}\right\|^2+\frac{\delta_k^2}{\theta_k}-v_k\leqslant 0,\forall k\in\mathcal{K} \tag{10c}$$

$$\frac{E_k}{(1-\theta_k)}-\left(\text{Tr}\left(\mathbf{T}_k\mathbf{W}\right)+\sigma_z^2\left\|\mathbf{h}_k^H\mathbf{\Psi}\mathbf{R}\right\|^2\right)\leqslant 0,\forall k\in\mathcal{K} \tag{10d}$$

$$\text{Tr}\left(\mathbf{W}\right)-P_{\text{Tx}}\leqslant 0 \tag{10e}$$

$$\text{Tr}\left(\left(\mathbf{\Psi}\mathbf{R}\mathbf{G}\right)^H\left(\mathbf{\Psi}\mathbf{R}\mathbf{G}\right)\mathbf{W}\right)+\sigma_z^2\|\mathbf{\Psi}\mathbf{R}\|^2-P_{\text{I}}\leqslant 0 \tag{10f}$$

$$1\geqslant\theta_k\geqslant 0,\ \ \forall k\in\mathcal{K} \tag{10g}$$

$$u_k\geqslant 0, v_k\geqslant 0,\ \forall k\in\mathcal{K} \tag{10h}$$

$$\mathbf{W}\succeq 0 \tag{10i}$$

$$\text{rank}\,(\mathbf{W})=1. \tag{10j}$$

Since $\mathbf{W}$ is positive semidefinite matrix (10i), the rank-one constraint (10j) is equivalently expressed as $\text{Tr}\,(\mathbf{W})-\lambda_1(\mathbf{W})\leqslant 0$, where λ_1 is maximum eigenvalue of $\mathbf{W}$. Then via the exact penalty function method [37], we move the novel condition into the objective to formulate the penalty function with a large enough penalty parameter κ as:

$$\max_{\substack{\mathbf{W},\theta_k,\\ u_k,v_k}}\ \sum_{k=1}^{K}\left[\log_2\left(v_k+u_k+\sigma_k^2\right)-\log_2\left(v_k+\sigma_k^2\right)\right] -\kappa\left(\text{Tr}\left(\mathbf{W}\right)-\lambda_1\left(\mathbf{W}\right)\right)$$

We use Taylor approximation for the concave function:

$$\log_2\left(v_k+\sigma_k^2\right)\leqslant\left(\begin{array}{l}\log_2\left(v_k^{(l)}+\sigma_k^2\right)+\\ \frac{1}{\ln 2\cdot\left(v_k^{(l)}+\sigma_k^2\right)}\left(v_k-v_k^{(l)}\right)\end{array}\right). \tag{11}$$

Moreover, the convex function $\lambda_1(\mathbf{W})$ has a subgradient $\mathbf{q}_1\mathbf{q}_1^H$ with the unit-norm eigenvector $\mathbf{q}_1$ corresponding the maximum eigenvalue λ_1 [38]:

$$\lambda_1(\mathbf{W})\geqslant\lambda_1\left(\mathbf{W}^{(l)}\right)+\mathbf{q}_1^{(l)H}\left(\mathbf{W}-\mathbf{W}^{(l)}\right)\mathbf{q}_1^{(l)}=\mathbf{q}_1^{(l)H}\mathbf{W}\mathbf{q}_1^{(l)}. \tag{12}$$

Then, at the fixed point

$$\left\{v_k^{(l)},\mathbf{W}^{(l)},\lambda_1\left(\mathbf{W}^{(l)}\right),\mathbf{q}_1^{(l)}\right\}$$

the convex optimization subproblem is rewritten as follows:

$$\max_{\substack{\mathbf{W},\theta_k,\\ u_k,v_k\}}}\ \sum_{k=1}^{K}\left[\begin{array}{l}\log_2\left(v_k+u_k+\sigma_k^2\right)-\\ \left(\begin{array}{l}\log_2\left(v_k^{(l)}+\sigma_k^2\right)+\\ \frac{1}{\ln 2\cdot\left(v_k^{(l)}+\sigma_k^2\right)}\left(v_k-v_k^{(l)}\right)\end{array}\right)\end{array}\right] -\kappa\left(\text{Tr}\left(\mathbf{W}\right)-\mathbf{q}_1^{(l)H}\mathbf{W}\,\mathbf{q}_1^{(l)}\right) \tag{13a}$$

$$\text{s.t.: (10b), ..., (10i).} \tag{13b}$$

Therefore, this convex optimization problem may be solved by the Matlab CVX tool [36]. Then, the optimal solution of this convex optimization problem is used to update the fixed point

$$\left\{v_k^{(l)},\mathbf{W}^{(l)},\lambda_1\left(\mathbf{W}^{(l)}\right),\mathbf{q}_1^{(l)}\right\}$$

and the procedure is repeated until satisfying the convergent conditions. To find a point for the initialization, we solve the problem as:

$$\underset{\{\mathbf{W},\theta_k\}}{\text{maximize}}\ \ 0 \tag{14a}$$

$$\text{subject to:}\ \ \text{(10d), (10e), (10f), (10g), (10i).} \tag{14b}$$

The optimal solution of the problem is assigned for $\left\{\mathbf{W}^{(0)},\theta_k^{(0)}\right\}$, then $\left\{v_k^{(0)}\right\}$ is obtained as

$$v_k^{(0)}=\sigma_z^2\left\|\mathbf{h}_k^H\mathbf{\Psi}\mathbf{R}\right\|^2+\frac{\delta_k^2}{\theta_k^{(0)}},\ \forall k\in\mathcal{K}.$$

Algorithm 1 The proposed algorithm with the SDR-based approach to optimize the spectral efficiency of problem (5).

1: **Initialization:** Starting fixed phase shifts $\{\varphi_n\}$, active IRS element power, $\{b_n\}$, largest iteration number, I_1
2: **For** $l=1$ **to** I_1 **do**
3: Solving problem (14) to achieve the initial feasible SCA point
4: Solving problem (13) with SDR-based method to achieve $\{\mathbf{W}^*,\theta_k^*,v_k^*,\mathbf{q}_1^*\}$ with fixed $\{b_n,\varphi_n\}$
5: Update $\left\{v_k^{(l)},\mathbf{q}_1^{(l)}\right\}\leftarrow\{v_k^*,\mathbf{q}_1^*\}$
6: **If** accuracy is obtained **then**
7: Break
8: **End If**
9: **End For**
10: **Output:** Optimal solution $\{\mathbf{w},\theta_k\}\leftarrow\{\mathbf{w}^*,\theta_k^*\}$, optimal value $\sum_{k=1}^{K}\log_2\left(1+\frac{\left|\left(\mathbf{t}_k^H+\mathbf{h}_k^H\mathbf{\Psi}\mathbf{R}\mathbf{G}\right)\mathbf{w}\right|^2}{\sigma_z^2\left\|\mathbf{h}_k^H\mathbf{\Psi}\mathbf{R}\right\|^2+\sigma_k^2+\frac{\delta_k^2}{\theta_k}}\right)$

3.2. Solving Subproblem of Active IRS Parameters

Next, we find the amplification factors and the phase shifts at the active IRS when the beamforming vector and the PS

factor are fixed. We consider (P3) as follows:

$$\max_{\{b_n,\varphi_n\}} \ 0 \tag{15a}$$

$$\text{s.t.:} \left|\left(\mathbf{t}_k^H + \mathbf{h}_k^H \mathbf{\Psi R G}\right)\mathbf{w}\right|^2 \geqslant u_k,\ \forall k \in \mathcal{K} \tag{15b}$$

$$\sigma_z^2 \left\|\mathbf{h}_k^H \mathbf{\Psi R}\right\|^2 + \frac{\delta_k^2}{\theta_k} \leqslant v_k,\ \forall k \in \mathcal{K} \tag{15c}$$

$$\left(\begin{array}{l}\left|\left(\mathbf{t}_k^H + \mathbf{h}_k^H \mathbf{\Psi R G}\right)\mathbf{w}\right|^2 \\ +\sigma_z^2 \left\|\mathbf{h}_k^H \mathbf{\Psi R}\right\|^2\end{array}\right) \geqslant \frac{E_k}{(1-\theta_k)}, \forall k \in \mathcal{K} \tag{15d}$$

$$\|\mathbf{\Psi RGw}\|^2 + \sigma_z^2 \|\mathbf{\Psi R}\|^2 \leqslant P_1. \tag{15e}$$

For constraint (15b), we denote

$$\mathbf{f} = \left[b_1 e^{j\varphi_1}, b_2 e^{j\varphi_2}, \cdots, b_N e^{j\varphi_N}\right]^H \in \mathbb{C}^{N\times 1}$$

and thus derive

$$\mathbf{h}_k^H \mathbf{\Psi RGw} = \mathbf{f}^H diag\left(\mathbf{h}_k^H\right)\mathbf{Gw}\ .$$

we rewrite as:

$$\left|\left(\mathbf{t}_k^H + \mathbf{h}_k^H \mathbf{\Psi RG}\right)\mathbf{w}\right|^2 = \left|\mathbf{f}^H diag\left(\mathbf{h}_k^H\right)\mathbf{Gw} + \mathbf{t}_k^H \mathbf{w}\right|^2 . \tag{16}$$

With $\mathbf{x}_k = diag\left(\mathbf{h}_k^H\right)\mathbf{Gw}$, $y_k = \mathbf{t}_k^H \mathbf{w}$, we formulate:

$$\begin{aligned}\left|\mathbf{f}^H \mathbf{x}_k + y_k\right|^2 &= \left(\mathbf{f}^H \mathbf{x}_k + y_k\right)\left(\mathbf{f}^H \mathbf{x}_k + y_k\right)^H \\ &= \mathbf{f}^H \mathbf{x}_k \mathbf{x}_k^H \mathbf{f} + y_k \mathbf{x}_k^H \mathbf{f} + \mathbf{f}^H \mathbf{x}_k y_k^H + y_k^H y_k \\ &= [\mathbf{f}\ ,\ 1]^H \begin{bmatrix}\mathbf{x}_k \mathbf{x}_k^H & \mathbf{x}_k y_k^H \\ y_k \mathbf{x}_k^H & 0\end{bmatrix}\begin{bmatrix}\mathbf{f}\\ 1\end{bmatrix} + y_k^H y_k\ ,\end{aligned} \tag{17}$$

where

$$\mathbf{A}_1 = \begin{bmatrix}\mathbf{x}_k \mathbf{x}_k^H & \mathbf{x}_k y_k^H \\ y_k \mathbf{x}_k^H & 0\end{bmatrix}\ .$$

We assign $\mathbf{F} = \tilde{\mathbf{f}}\tilde{\mathbf{f}}^H$, $\tilde{\mathbf{f}} = [\mathbf{f}; 1]$, Then, constraint (15b) is rewritten as:

$$\mathrm{Tr}\left(\mathbf{A}_1 \mathbf{F}\right) + y_k^H y_k \geqslant u_k,\ \forall k.$$

For constraint (15c), first we transform as:

$$\begin{aligned}\left\|\mathbf{h}_k^H \mathbf{\Psi R}\right\|^2 &= \left\|\mathbf{f}^H diag\left(\mathbf{h}_k^H\right)\right\|^2 = \|diag\left(\mathbf{h}_k\right)\mathbf{f}\|^2 \\ &= \mathbf{f}^H diag\left(\mathbf{h}_k^H\right) diag\left(\mathbf{h}_k\right)\mathbf{f} = \mathbf{f}^H \mathbf{H}_k \mathbf{f} \\ &= \tilde{\mathbf{f}}^H \tilde{\mathbf{H}}_k \tilde{\mathbf{f}} = \mathrm{Tr}\left(\tilde{\mathbf{H}}_k \mathbf{F}\right)\end{aligned} \tag{18}$$

where:

$$\begin{aligned}\mathbf{H}_k &= diag\left(\mathbf{h}_k^H\right) diag\left(\mathbf{h}_k\right), \\ \tilde{\mathbf{H}}_k &= \left[\mathbf{H}_k, \mathbf{0}_{N\times 1}; \mathbf{0}_{1\times N}, 0\right].\end{aligned}$$

Then, constraint (15c) is converted as:

$$\sigma_z^2 \mathrm{Tr}\left(\tilde{\mathbf{H}}_k \mathbf{F}\right) + \frac{\delta_k^2}{\theta_k} \leqslant v_k,\ \forall k \in \mathcal{K}\ . \tag{19}$$

For constraint (15d), from equation (18) we derive the equivalent form as:

$$\mathrm{Tr}\left(\mathbf{A}_1 \mathbf{F}\right) + y_k^H y_k + \sigma_z^2 \mathrm{Tr}\left(\tilde{\mathbf{H}}_k \mathbf{F}\right) \geqslant \frac{E_k}{(1-\theta_k)},\ \forall k \in \mathcal{K}\ . \tag{20}$$

For constraint (15e), we transform the first term on the left side as:

$$\begin{aligned}\|\mathbf{\Psi RGw}\|^2 &= \left\|\mathbf{f}^H diag\left(\mathbf{Gw}\right)\right\|^2 \\ &= \mathbf{f}^H diag\left(\mathbf{Gw}\right)\left(diag\left(\mathbf{Gw}\right)\right)^H \mathbf{f} \\ &= \mathbf{f}^H \bar{\mathbf{G}} \mathbf{f} \\ &= \tilde{\mathbf{f}}^H \tilde{\mathbf{G}} \tilde{\mathbf{f}} = \mathrm{Tr}\left(\tilde{\mathbf{G}}\mathbf{F}\right)\end{aligned}, \tag{21}$$

where:

$$\bar{\mathbf{G}} = diag\left(\mathbf{Gw}\right)\left(diag\left(\mathbf{Gw}\right)\right)^H\ ,$$

$$\tilde{\mathbf{G}} = \left[\bar{\mathbf{G}}, \mathbf{0}_{N\times 1}; \mathbf{0}_{1\times N}, 0\right]\ .$$

Moreover, the second term is expressed as:

$$\|\mathbf{\Psi R}\|^2 = \|\mathbf{f}\|^2 = \left\|\tilde{\mathbf{f}}\right\|^2 - 1 = \tilde{\mathbf{f}}^H \tilde{\mathbf{f}} - 1 = \mathrm{Tr}\left(\mathbf{F}\right) - 1\ . \tag{22}$$

Similar to (12), the rank-one condition is approximated by:

$$\lambda_1\left(\mathbf{F}\right) \geqslant \lambda_1\left(\mathbf{F}^{(i)}\right) + \mathbf{e}_1^{(i)H}\left(\mathbf{F} - \mathbf{F}^{(i)}\right)\mathbf{e}_1^{(i)} = \mathbf{e}_1^{(i)H}\mathbf{F}\mathbf{e}_1^{(i)}\ . \tag{23}$$

The final problem is expressed as:

$$\min_{\{\mathbf{F}\}} \left(\mathrm{Tr}\left(\mathbf{F}\right) - \mathbf{e}_1^{(i)H}\mathbf{F}\mathbf{e}_1^{(i)}\right) \tag{24a}$$

$$\text{s.t.:}\ \mathrm{Tr}\left(\mathbf{A}_1\mathbf{F}\right) + y_k^H y_k \geqslant u_k,\ \forall k \in \mathcal{K} \tag{24b}$$

$$\sigma_z^2 \mathrm{Tr}\left(\tilde{\mathbf{H}}_k \mathbf{F}\right) + \frac{\delta_k^2}{\theta_k} \leqslant v_k,\ \forall k \in \mathcal{K} \tag{24c}$$

$$\left(\begin{array}{l}\mathrm{Tr}\left(\mathbf{A}_1\mathbf{F}\right) + y_k^H y_k \\ +\sigma_z^2 \mathrm{Tr}\left(\tilde{\mathbf{H}}_k \mathbf{F}\right)\end{array}\right) \geqslant \frac{E_k}{(1-\theta_k)},\ \forall k \in \mathcal{K} \tag{24d}$$

$$\mathrm{Tr}\left(\tilde{\mathbf{G}}\mathbf{F}\right) + \sigma_z^2\left(\mathrm{Tr}\left(\mathbf{F}\right) - 1\right) \leqslant P_1. \tag{24e}$$

To start at an initial feasible point, we solve the SDP problem to obtain $\mathbf{e}_1^{(0)}$ as follows:

$$\underset{\{\mathbf{F}\}}{\text{minimize}}\ \ 0 \tag{25a}$$

$$\text{subject to}\ \ (24b), (24c), (24d), (24e). \tag{25b}$$

Then, the initial values for variables $\mathbf{F}^{(0)}$ and $\mathbf{e}_1^{(0)}$ are obtained by the optimal solution. After that, the detailed solution is presented as Algorithm 2.

Finally, the proposed iterative algorithm is illustrated via flowchart form in Fig. 2 and the detailed steps in Algorithm 3.

4. Numerical Experiments

In this part of the paper, the numerical experiments of the iterative algorithm designed for solving the transceiver and active IRS subproblems and the total system problem are presented to evaluate the effect of the proposed method.

For setting system parameters similar to [10], [39], the hybrid user number is assigned $K = 3$, the noise powers of the active IRS and the PS hybrid users are $\sigma_{\mathrm{I}}^2 = -40$ dBm, $\sigma_k^2 = -50$ dBm, and $\delta_k^2 = -40$ dBm, $\forall k \in \mathcal{K}$. The distance-dependent pathloss for every link is expressed as $PL = [-30 - 10\,\beta \log_{10}(d)]$ dB, where is the path loss at

Algorithm 2 The iterative algorithm with the SDR-based approach to achieve optimal amplification and phase shifts coefficients.

Initialization: Fixed $\{\mathbf{w}, \theta_k, u_k, v_k\}$, setting iteration number, I_2
Finding initial values for variables $\mathbf{F}^{(0)}$ and $\mathbf{e}_1^{(0)}$ by solving the initial problem (25)
For $l = 1$ **to** I_2 **do**
  Solving tractable convex problem (24) with SDR-based method to achieve $\mathbf{F}^*$ and $\mathbf{e}_1^*$
  Update $\left\{\mathbf{F}^{(i)}, \mathbf{e}_1^{(i)}\right\} \leftarrow \{\mathbf{F}^*, \mathbf{e}_1^*\}$
  If accuracy is obtained **then**
    Break
  End If
End For
Decompose: $\mathbf{F}^{(i)} = \tilde{\mathbf{f}}^{(i)}\tilde{\mathbf{f}}^{(i)H}$
Derive $\mathbf{f}^{(i)} = \left[\tilde{\mathbf{f}}^{(i)}\right]_{1:N} / \tilde{f}_{N+1}^{(i)}$ and phase-shift coefficients $\varphi_n^{(i)} = -\arg\left(f_n^{(i)}\right), \forall n \in \mathcal{N}$, amplification coefficients $b_n^{(i)} = \left|f_n^{(i)}\right|, \forall n \in \mathcal{N}$
Output: optimal solution $\{b_n, \varphi_n\} \leftarrow \left\{b_n^{(i)}, \varphi_n^{(i)}\right\}$

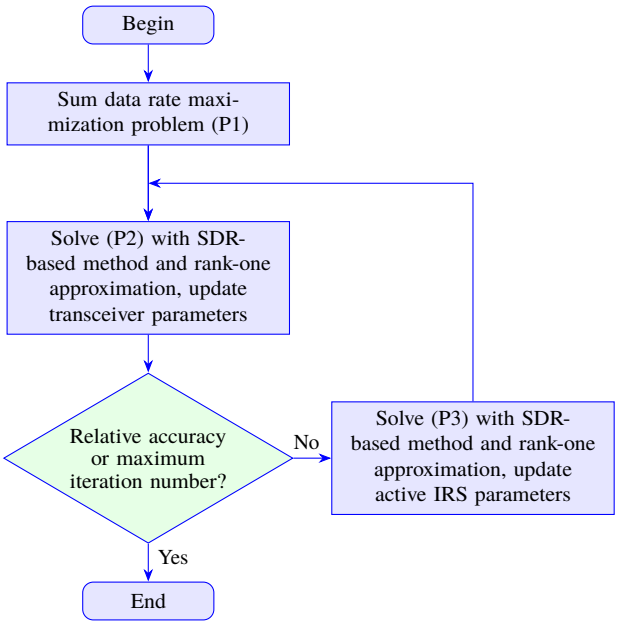

Fig. 2. Particle swarm optimization flow chart.

the reference distance –30 dB, d denotes the link range, and β indicates the pathloss factor. The factor β is allotted 2.2 for the links of BS-active IRS and active IRS-users, and 3.8 for the links of BS-users.

We apply the Rician fading formula for the small-scale model with the Rician coefficient $K_R = 3$ dB. The BS location is placed at (0 m, 0 m) and the active IRS is placed at (3 m, 2.5 m). Moreover, the hybrid user locations are uniformly placed at the circle which has the centre point (6 m, 0 m) and the radius 0.5 m.

We apply the Rician fading formula for the small-scale model with the Rician coefficient of $K_R = 3$ dB. The BS is placed

Algorithm 3 The final iterative algorithm for optimizing the transceivers and active IRS parameters.

Initialization: Starting initial phase-shift coefficients $\left\{\varphi_n^{(0)}\right\}$, active amplification coefficients, $\left\{b_n^{(0)}\right\}$, largest number of iterations, I_3
Finding initial values for variables $\mathbf{F}^{(0)}$ and $\mathbf{e}_1^{(0)}$ by solving the initial problem (25)
For $p = 1$ **to** I_3 **do**
  Solving problem (5) via SDR-based approach to achieve $\left\{\mathbf{w}^{(p)}, \theta_k^{(p)}\right\}$ under the given active IRS parameters
  Solving problem (15) via SDR-based approach to achieve $\left\{b_n^{(p)}, \varphi_n^{(p)}\right\}$ under the given transceiver parameters
  If accuracy is obtained **then**
    Break
  End If
End For
Output: optimal solution
$\{\mathbf{w}, \theta_k, b_n, \varphi_n\} \leftarrow \left\{\mathbf{w}^{(p)}, \theta_k^{(p)}, b_n^{(p)}, \varphi_n^{(p)}\right\}$,
and optimal value
$$\sum_{k=1}^{K} \log_2\left(1 + \frac{\left|\left(\mathbf{t}_k^H + \mathbf{h}_k^H \boldsymbol{\Psi}\mathbf{R}\mathbf{G}\right)\mathbf{w}\right|^2}{\sigma_z^2\left\|\mathbf{h}_k^H \boldsymbol{\Psi}\mathbf{R}\right\|^2 + \sigma_k^2 + \frac{\delta_k^2}{\theta_k}}\right)$$

at (0 m, 0 m) and the active IRS is placed at (3 m, 2.5 m). Moreover, the hybrid user locations are uniformly placed along a circle with a center point of (6 m, 0 m) and a radius of 0.5 m.

Figure 3 expresses the iteration results of the SDR-based iterative procedure completed using Algorithm 2 under several fixed phase shifts and amplification coefficients of the active intelligent surface. The subproblem (13) provides the target result which rises and goes to the fixed value with lower five repetitions. In addition, the result of $\left(\mathrm{Tr}\left(\mathbf{W}\right) - \mathbf{z}_1^{(l)H}\mathbf{W}\mathbf{z}_1^{(l)}\right)$ is approximate zero with the high value penalty coefficient κ. Consequently, SDR-based formula of rank-1 condition is satisfied, then the BS beamforming solution is obtained via decomposition technique.

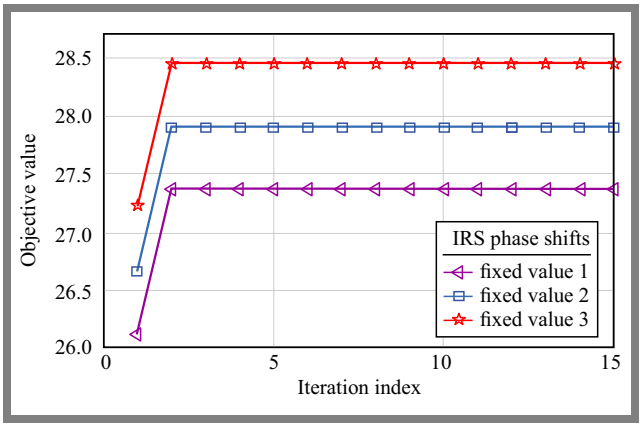

Fig. 3. Convergent behavior of proposed iterative Algorithm 1.

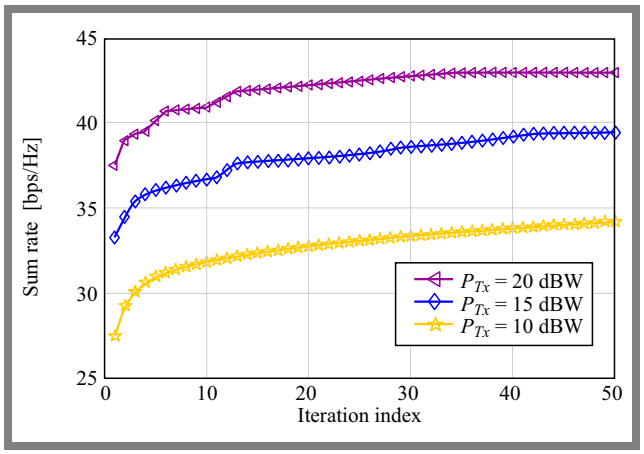

Fig. 4. Convergent behavior of proposed iterative Algorithm 3.

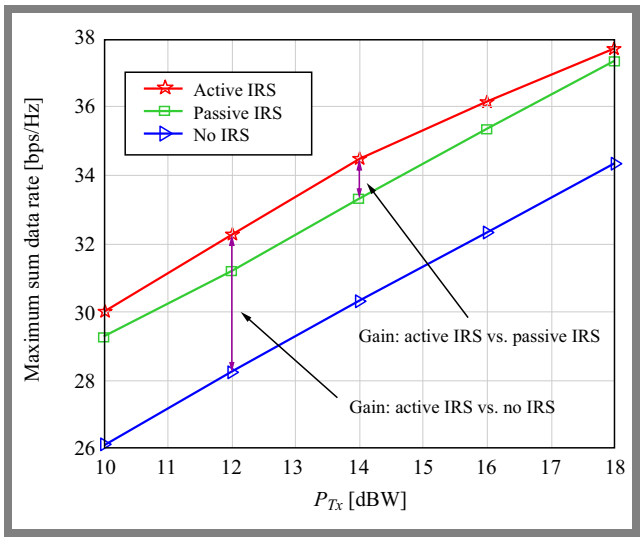

Fig. 5. Maximum sum data rate versus BS transmission power.

Figure 4 expresses the iteration results of the proposed alternating optimization Algorithm 3 under some BS transmission power values. As seen in Fig. 3, the sum data rate increases gradually after each iteration until convergence is achieved. Then, we set the largest iteration of AO iteration number is $I_3 = 50$ and the relative accuracy is $\Delta = 10^{-2}$ for terminating loop.

Figure 5 presents the maximum sum data rate via BS transmission power for three schemes, including the proposed active IRS, passive IRS, and a solution without IRS, when the number of BS antennas is $M = 5$, number of IRS components is $N = 10$, active IRS power is $P_I = 5$ dBW, and the required energy harvesting threshold is $E_k = -25$ dBm.

We observe that the support of active IRS provides the highest total sum rate in comparison with a scenario with passive IRS and a solution without IRS schemes. For instance, when $P_{\mathrm{Tx}} = 12$ dBW, the proposed active IRS scheme achieves 32.23 bps/Hz, while the passive IRS and the solution without IRS obtain 31.21 bps/Hz and 28.24 bps/Hz, respectively. Furthermore, the increase of maximum BS power provides a higher total sum rate.

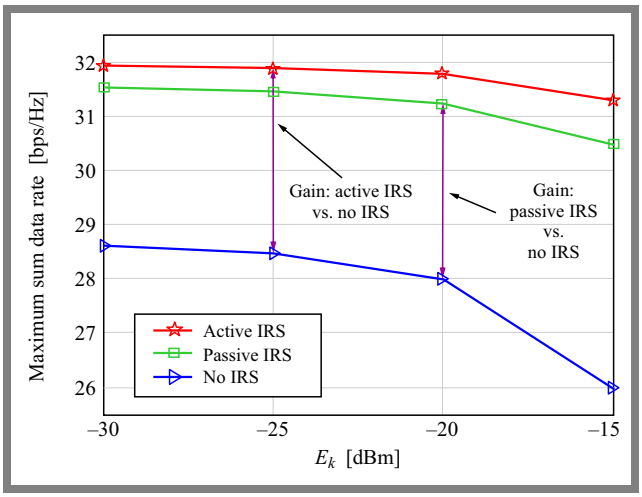

Fig. 6. Maximum sum data rate versus required energy harvesting value.

Figure 6 presents the maximum sum data rate via the required EH value, E_k in three schemes, including the proposed active IRS, passive IRS, and a scheme without IRS, when the number of BS antennas is $M = 8$, number of IRS components is $N = 10$, active IRS power is $P_I = 1$ dBW, and maximum BS power is $P_{\mathrm{Tx}} = 10$ dBW.

It can be observed that the sum data rate of PS hybrid users goes down with the increase of the required EH threshold. The reason is that when the EH threshold is higher, PS hybrid users have to split more energy for EH circuits, and then keep less energy for decoding data. In addition, the result of the considered active IRS scheme is also higher than that of the passive IRS and the scheme without IRS when both amplification and phase-shift coefficients are optimized.

5. Conclusions

In this study, the total data rate optimization for SWIPT with PS hybrid users and an active IRS aid is investigated via an SDR-based approach, rank-one approximations, and AO method. The SDR-based iterative algorithm shows fast convergence with a few iterations. Under the impact of amplification characteristics, the sum rate result of the active IRS-assisted scheme is better than that of the passive IRS-assisted SWIPT with only phase shifts and the solution scheme without IRS.

Moreover, the sum rate results are higher with an increase in the number of BS antennas, number of IRS components or BS transmission power. In conclusion, future research should focus on rendering the system more robust under the influence of imperfect channel-side information of the active IRS.

Acknowledgments

This research is funded by University of Education, Hue University, under grant number NCTB-T.24-TN.103.02. This research is funded by Vietnam National Foundation for Science and Technology Development (NAFOSTED), under grant number 102.04-2023.40.

Appendix A: Proof that problems (4) and (5) have the same maximum value

We denote the objective functions of problems (4) and (5) as $f_4\left(\mathbf{w}, \theta_k\right)$ and $f_5\left(\mathbf{w}, \theta_k, u_k, v_k\right)$, respectively.

We assume that the maximum values of problems (4) and (5) are $P^*_{(4)}$ at $\{\mathbf{w}^*, \theta^*_k\}$ and $P^*_{(5)}$ at $\{\tilde{\mathbf{w}}^*, \tilde{\theta}^*_k, \tilde{u}^*_k, \tilde{v}^*_k\}$, respectively. We have:

$$\begin{aligned} P^*_{(5)} &= f_5\left(\tilde{\mathbf{w}}^*, \tilde{\theta}^*_k, \tilde{u}^*_k, \tilde{v}^*_k\right) \leqslant f_4\left(\tilde{\mathbf{w}}^*, \tilde{\theta}^*_k\right) \\ &\leqslant f_4\left(\mathbf{w}^*, \theta^*_k\right) = P^*_{(4)} \end{aligned} \tag{26}$$

due to (5a), (5b), and (5c). Conversely, we have:

$$\begin{aligned} P^*_{(4)} &= f_4\left(\mathbf{w}^*, \theta^*_k\right) = f_5\left(\mathbf{w}^*, \theta^*_k, u^\dagger_k, v^\dagger_k\right) \\ &\leqslant f_5\left(\tilde{\mathbf{w}}^*, \tilde{\theta}^*_k, \tilde{u}^*_k, \tilde{v}^*_k\right) = P^*_{(5)} \end{aligned} \tag{27}$$

where

$$u^\dagger_k = \left|\left(\mathbf{t}^H_k + \mathbf{h}^H_k \mathbf{\Psi R G}\right)\mathbf{w}^*\right|^2$$

and

$$v^\dagger_k = \sigma^2_z \left\|\mathbf{h}^H_k \mathbf{\Psi R}\right\|^2 + \frac{\delta^2_k}{\theta^*_k}, \forall k \in \mathcal{K}$$

Therefore, we conclude $P^*_{(4)} = P^*_{(5)}$.

References

[1] I. Krikidis *et al.*, "Simultaneous Wireless Information and Power Transfer in Modern Communication Systems", *IEEE Communications Magazine*, vol. 52, pp. 104–110, 2014 (https://doi.org/10.1109/MCOM.2014.6957150).

[2] C. Psomas *et al.*, "Wireless Information and Energy Transfer in the Era of 6G Communications", *Proceedings of the IEEE*, vol. 112, pp. 764–804, 2024 (https://doi.org/10.1109/JPROC.2024.3395178).

[3] T.D.P. Perera *et al.*, "Simultaneous Wireless Information and Power Transfer (SWIPT): Recent Advances and Future Challenges", *IEEE Communications Surveys & Tutorials*, vol. 20, pp. 264–302, 2017 (https://doi.org/10.1109/COMST.2017.2783901).

[4] Z. Kang, C. You, and R. Zhang, "Active-IRS-aided Wireless Communication: Fundamentals, Designs and Open Issues", *IEEE Wireless Communications*, vol. 31, pp. 368–374, 2024 (https://doi.org/10.1109/MWC.003.2300013).

[5] Z. Peng *et al.*, "Beamforming Optimization for Active RIS-aided Multiuser Communications with Hardware Impairments", *IEEE Transactions on Wireless Communications*, vol. 23, pp. 9884–9898, 2024 (https://doi.org/10.1109/TWC.2024.3367131).

[6] R. Patra and A. Mahapatro, "Reconfigurable Intelligent Surface-based Propagation Control in FBMC/OQAM Systems", *Journal of Telecommunications and Information Technology*, vol. 95, pp. 83–90, 2024 (https://doi.org/10.26636/jtit.2024.1.1326).

[7] J. Tang *et al.*, "Energy Efficiency Optimization for a ultiuser IRS-aided MISO System with SWIPT", *IEEE Transactions on Communications*, vol. 71, pp. 5950–5962, 2023 (https://doi.org/10.1109/TCOMM.2023.3296631).

[8] M.R. Camana, C.E. Garcia, and I. Koo, "Rate-splitting Multiple Access in a MISO SWIPT System Assisted by an Intelligent Reflecting Surface", *IEEE Transactions on Green Communications and Networking*, vol. 6, pp. 2084–2099, 2022 (https://doi.org/10.1109/TGCN.2022.3196048).

[9] Q. Wu and R. Zhang, "Weighted Sum Power Maximization for Intelligent Reflecting Surface Aided SWIPT", *IEEE Wireless Communications Letters*, vol. 9, pp. 586–590, 2019 (https://doi.org/10.1109/LWC.2019.2961656).

[10] P.V. Tuan, M.T. Le, T.T. Duy, and I. Koo, "An SDR-based Approach for Efficient Simultaneous Wireless Information Power Transfer with Active IRS Assistance", *Proc. of International Conference on Industrial Networks and Intelligent Systems*, pp. 57–66, 2025 (https://doi.org/10.1007/978-3-032-02362-9_5).

[11] Y. Shen *et al.*, "Outage Constrained Max-min Secrecy Rate Optimization for IRS-aided SWIPT Systems with Artificial Noise", *IEEE Internet of Things Journal*, vol. 11, pp. 9814–9828, 2023 (https://doi.org/10.1109/JIOT.2023.3325362).

[12] J. Liu *et al.*, "Energy Efficiency in Secure IRS-aided SWIPT", *IEEE Wireless Communications Letters*, vol. 9, pp. 1884–1888, 2020 (https://doi.org/10.1109/LWC.2020.3006837).

[13] Z. Li *et al.*, "Joint Beamforming Design and Power Splitting Optimization in IRS-assisted SWIPT NOMA Networks", *IEEE Transactions on Wireless Communications*, vol. 21, pp. 2019–2033, 2021 (https://doi.org/10.1109/TWC.2021.3108901).

[14] M.B. Goktas, Y. Dursun, and Z. Ding, "IRS and SWIPT-assisted Full-duplex NOMA for 6G umMTC", *IEEE Transactions on Green Communications and Networking*, vol. 7, pp. 1957–1970, 2023 (https://doi.org/10.1109/TGCN.2023.3289505).

[15] Y. Gao *et al.*, "Beamforming Optimization for Active Intelligent Reflecting Surface-aided SWIPT", *IEEE Transactions on Wireless Communications*, vol. 22, pp. 362–378, 2022 (https://doi.org/10.1109/TWC.2022.3193845).

[16] Q. Zhai, L. Dong, Y. Li, and W. Cheng, "Secure Communications via Active IRS Assisted SWIPT NOMA Networks", *IEEE Systems Journal*, vol. 18, pp. 1032–1043, 2024 (https://doi.org/10.1109/JSYST.2024.3365590).

[17] A.B. Gershman *et al.*, "Convex Optimization-based Beamforming", *IEEE Signal Processing Magazine*, vol. 27, pp. 62–75, 2010 (https://doi.org/10.1109/MSP.2010.936015).

[18] A.M. Elbir, K.V. Mishra, S.A. Vorobyov, and R.W. Heath, "Twenty-five Years of Advances in Beamforming: From Convex and Nonconvex Optimization to Learning Techniques", *IEEE Signal Processing Magazine*, vol. 40, pp. 118–131, 2023 (https://doi.org/10.1109/MSP.2023.3262366).

[19] H. Han *et al.*, "Reconfigurable Intelligent Surface Aided Power Control for Physical-layer Broadcasting", *IEEE Transactions on Communications*, vol. 69, pp. 7821–7836, 2021 (https://doi.org/10.1109/TCOMM.2021.3104871).

[20] A. Mohamed, A. Zappone, and M. Di Renzo, "Bi-objective Optimization of Information Rate and Harvested Power in RIS-aided SWIPT Systems", *IEEE Wireless Communication Letter,* vol. 11, pp. 2195–2199, 2022 (https://doi.org/10.1109/LWC.2022.3196906).

[21] S. Zargari, A. Hakimi, C. Tellambura, and S. Herath, "Multiuser MISO PS-SWIPT Systems: Active or Passive RIS?", *IEEE Wireless Communications Letters*, vol. 11, pp. 1920–1924, 2022 (https://doi.org/10.1109/LWC.2022.3187671).

[22] Z. Yang and Y. Zhang, "Optimal SWIPT in RIS-aided MIMO Networks", *IEEE Access*, vol. 9, pp. 112552–112560, 2021 (https://doi.org/10.1109/ACCESS.2021.3099698).

[23] S. Faramarzi *et al.*, "Energy Efficient Design of Active STAR-RIS-aided SWIPT Systems", *IEEE Transactions on Wireless Communications*, vol. 24, pp. 3209–3224, 2025 (https://doi.org/10.1109/TWC.2025.3528959).

[24] C. You and R. Zhang, "Wireless Communication Aided by Intelligent Reflecting Surface: Active or Passive?", *IEEE Wireless Communications Letters*, vol. 10, pp. 2659–2663, 2021 (https://doi.org/10.1109/LWC.2021.3111044).

[25] Z. Zhang *et al.*, "Active RIS vs. Passive RIS: Which Will Prevail in 6G?", *IEEE Transactions on Communications*, vol. 71, pp. 1707–1725, 2023 (https://doi.org/10.1109/TCOMM.2022.3231893).

[26] R. Zhang and C.K. Ho, "MIMO Broadcasting for Simultaneous Wireless Information and Power Transfer", *IEEE Transactions on Wireless Communications*, vol. 12, pp. 1989–2001, 2013 (https://doi.org/10.1109/TWC.2013.031813.120224).

[27] Y. Wu *et al.*,"Analytical Design Method of Multiway Dual-band Planar Power Dividers with Arbitrary Power Division", *IEEE Transactions on Microwave Theory and Techniques*, vol. 58, pp. 3832–3841, 2010 (https://doi.org/10.1109/TMTT.2010.2086712).

[28] Agilent 11667A,B power splitters, Agilent RF and Microwave Test Accessories, (https://www.testequipmenthq.com/datasheets/Keysight-11667A-Datasheet.pdf).

[29] C. He *et al.*, "A Novel Dual-band Power Divider with Controllable Power Ratio and Phase Difference", *IEEE Access*, vol. 12, pp. 153146–153153, 2024 (https://doi.org/10.1109/ACCESS.2024.3480134).

[30] S. Trovarello, G. Paolini, D. Masotti, and A. Costanzo, "A Modular System of Rectifiers for Energy Harvesting with Wide Dynamic Input-range", *2021 6th International Conference on Smart and Sustainable Technologies (SpliTech)*, Bol and Split, Croatia, 2021 (https://doi.org/10.23919/SpliTech52315.2021.9566459).

[31] E. Boshkovska, D.W.K. Ng, N. Zlatanov, and R. Schober, "Practical Non-linear Energy Harvesting Model and Resource Allocation for SWIPT Systems", *IEEE Communications Letters*, vol. 19, pp. 2082–2085, 2015 (https://doi.org/10.1109/LCOMM.2015.2478460).

[32] Q. Wu and R. Zhang, "Joint Active and Passive Beamforming Optimization for Intelligent Reflecting Surface Assisted SWIPT Under QoS Constraints", *IEEE Journal on Selected Areas in Communications*, vol. 38, pp. 1735–1748, 2020 (https://doi.org/10.1109/JSAC.2020.3000807).

[33] C. Psomas *et al.*, "Wireless Information and Energy Transfer in the Era of 6G Communications", *Proceedings of the IEEE*, vol. 112, pp. 764–804, 2024 (https://doi.org/10.1109/JPROC.2024.3395178).

[34] R. Long, Y.-C. Liang, Y. Pei, and E.G. Larsson, "Active Reconfigurable Intelligent Surface Aided Wireless Communications", *IEEE Transactions on Wireless Communications*, vol. 20, pp. 4962–4975, 2021 (https://doi.org/10.1109/TWC.2021.3064024).

[35] Z.-Q. Luo *et al.*, "Semidefinite Relaxation of Quadratic Optimization Problems", *IEEE Signal Processing Magazine*, vol. 27, pp. 20–34, 2010 (https://doi.org/10.1109/MSP.2010.936019).

[36] M. Grant and S. Boyd, "CVX: Matlab Software for Disciplined Convex Programming, version 2.2", CVX Research, 2020 (https://cvxr.com/cvx/).

[37] S. Boyd and L. Vandenberghe, *Convex Optimization*, Cambridge University Press, 727 p., 2004 (ISBN 9780521833783).

[38] A.H. Phan, H.D. Tuan, H.H. Kha, and D.T. Ngo, "Nonsmooth Optimization for Efficient Beamforming in Cognitive Radio Multicast Transmission", *IEEE Transactions on Signal Processing*, vol. 60, pp. 2941–2951, 2012 (https://doi.org/10.1109/TSP.2012.2189857).

[39] Q. Wu and R. Zhang, "Intelligent Reflecting Surface Enhanced Wireless Network via Joint Active and Passive Beamforming", *IEEE Transactions on Wireless Communications*, vol. 18, pp. 5394–5409, 2019 (https://doi.org/10.1109/TWC.2019.2936025).

[40] P.V. Tuan, V.-Q.-B. Ngo, P. N. Son, and V.H. Vu, "An Energy Harvesting Fairness Maximization for Active/passive IRS-assisted PS-SWIPT System", *International Journal of Ad Hoc and Ubiquitous Computing*, vol. 49, pp. 215–224, 2025 (https://doi.org/10.1504/IJAHUC.2025.147751).

Pham Viet Tuan, Ph.D.
Faculty of Physics
https://orcid.org/0000-0002-7060-2272
E-mail: phamviettuan@dhsphue.edu.vn
E-mail: pvtuan@huenuni.edu.vn
University of Education, Hue University, Hue City, Vietnam
https://dhsphue.edu.vn

Hoang Dai Long, Ph.D.
Faculty of Electronics, Electrical Engineering and Material Technology
https://orcid.org/0000-0003-4056-6570
E-mail: hdlong@hueuni.edu.vn
University of Sciences, Hue University, Hue City, Vietnam
https://husc.edu.vn

Pham Ngoc Son, Associate Professor
Faculty of Electrical and Electronics Engineering
https://orcid.org/0000-0002-9698-4221
E-mail: sonpndtvt@hcmute.edu.vn
Ho Chi Minh City University of Technology and Engineering, Ho Chi Minh City, Vietnam
https://en.hcmute.edu.vn

Mai T.P. Le, Associate Professor
Faculty of Electronics and Telecommunication Engineering
https://orcid.org/0000-0001-9657-5172
E-mail: lpmai@dut.udn.vn
University of Science and Technology, The University of Danang, Da Nang City, Vietnam
https://en.dut.udn.vn